

# Fracture Behavior of Carbon-Epoxy under Different Loading

J. V. Sai Prasanna Kumar

**Abstract;** Delamination is the common failures of composite material attributed to various reasons, most importantly the potential stiffness degradation leading to small flaws and subsequently they propagate, and it becomes essential to characterize the new materials for interlaminar fracture. For the present study Carbon /epoxy system of IM7/8552 was investigated under mode I and mode II loading. Material was formed into unidirectional laminates with Teflon inserts at its mid length. The specimens were machined according to ASTM standards, Tests were executed on a quasi-static Instron 8225, with load control at 5 mm/min and 2 m/min for the mode -I and mode-II respectively. The strain energy release rate was found to be  $GIC=0.266 \text{ kJ/m}^2$  and  $GIIIC=0.687 \text{ kJ/m}^2$ . Fiberbridging was prominently absent in the DCB samples Examination of the fracture surface by SEM at SAIF, in IIT(M) and the nature of the fracture surface revealed the typical failure mechanism pertaining to mode-I and mode-II failure mechanisms.

**Keywords:** Mode-I, Mode-II, DCB, ENF, Fracture Toughness, SEM

## I. INTRODUCTION

Considerable amount research work was done on different types of loading either Mode I, Mode II or mixed- mode. Mode-I interlaminar received tremendous attention than any other mode because of inherent weakness of the interplay layer to delamination undergoing cleavage. Double cantilever beam (DCB) is the strong contender for these types of tests even though there is widely accepted standard exists for mode-I interlaminar fracture. Cleavage tests were adequate for many materials. Many researchers adopted and modified specimen introduced by Beery [2]. During mid 1960s number of authors were using fracture mechanics approach to examine the adhesive joints, the metal arms were suited to measure the strain energy release rate proved quite successful [3- 5]. Two types of samples which facilitated the premise that delamination must propagate along the mid plane: the straight edged beam and the tapered beam. A simple method is to attach the piano hinges and introduce a film in the mid plane as a starter crack. The sample could be straight or tapered edge. The dimensions of the hinges should be a minimum or else correction for moment arm must be made [6]. Then problem would be to provide starter crack, precracking was achieved with a razor [6] presently films are used to initiate the delamination. The layered composites are prone to crack initiation and subsequent propagation in the resin rich layers between plies. Delamination are introduced during processing or during service conditions.

This delamination can cause loss in stiffness of the component thus leading to failure of the structure and hence the composites are used in the empennage area of the aircraft where failure of the part is not so catastrophic. Attention now shifted to interlaminar shear mode-II fracture toughness study [7-9]. Several specimens were used to characterize the strain energy release rate in mode-II of which edge notched flexure (ENF) emerged as the most sought-after specimen to test to measure strain energy release rate in mode -II. The short beam shear(SBS) was the first test procedure introduced in 1960 [10-11], however it remains a quality control test measuring only the apparent interlaminar shear strength according to ASTM D-30 with the following dimensions:  $2L=100 \text{ mm}$ , width = 25 mm and thickness  $2h=3-4 \text{ mm}$ .

## II. DATA REDUCTION SCHEMES

The data reduction schemes for mode-I are broadly classified as compliance methods and energy methods. Numerous authors proposed expressions for the compliance and hence strain energy release rate [12] considering the crack tip geometry. Berry [3] started from beam theory and obtained expression for critical strain energy release rate and the empirical parameters would account for all the shear, rotation and crack tip response. For mode II specimens the data reduction starts from simple beam theory attributed to Gilliespie and Pipes [13], with materials having small thickness to crack length ratio the compliance for the ENF.

## III. MATERIALS AND TESTING METHODS

The experimental investigation of fracture toughness under Mode-I loading conditions have been e composite fibre IM7 and thermosetting epoxy matrix 8852 was considered for this investigation, the unidirectional Prepreg was obtained from S.B. Composites, Chennai. The prepregs were machined, laid in required sequence and were cured in autoclave. From the laminate the samples both DCB and ENF specimens were machined. Aluminum blocks were attached on the samples for DCB specimens which transfers load from the 100 KN loadcell to the specimen. These samples were mounted on the quasi-static Instron UTM figure 1. A total 10 samples were fabricated, a Teflon film of  $40 \mu$  was inserted in the mid-plane up to 40 mm in length.

Revised Manuscript Received on January 05, 2020.

J. V. Sai Prasanna Kumar, Department of Aeronautical Engineering, Vel Tech Rangarajan Dr. Sagunthala Institute of R& D Science and Technology Chennai-600062, India.

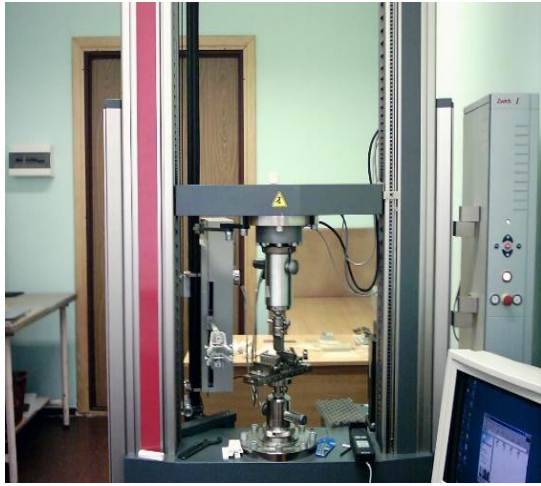


Figure 1 DCB sample mounted in UTM

The length of the sample was 192 mm 3mm thick and 25 mm wide with a cross head speed of 5 mm/min figure 2.



Figure 2 DCB Testing in progress

Out of the 10 samples and nine samples were tested. Seven samples in mode-II ENF samples were tested on three-point bending fixture with the quasi-static UTM at a crosshead speed of 2mm/ min at ambient atmospheric conditions figure 3

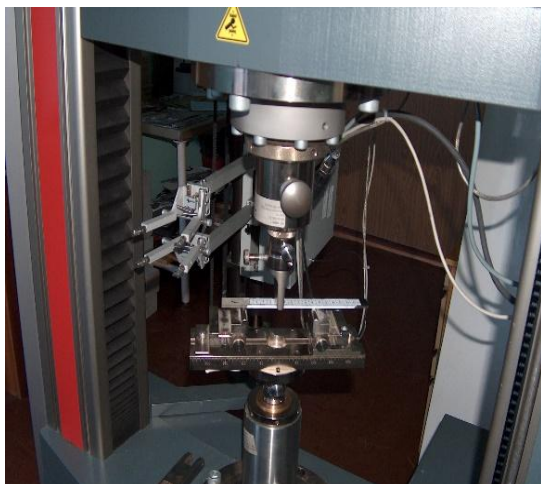


Figure 3 ENF Sample being tested

The overall dimensions of the ENF samples was 100 mmx 25 mmx 3mm. A Teflon film of length 40 mm was inserted in the mid-plane.

#### IV. RESULTS AND DISCUSSIONS

Nine DCB samples of different crack lengths were tested. The compliance was obtained from beam theory linear approximations were used to estimate the parameter from the slope of the compliance plot on logarithmic scale figure 4 and the value of  $n$  was 2.69. While the modulus was extracted from beam theory employing the experimental data for nine specimens and it was found to be  $140389.3\text{N/mm}^2$  and the moduli were  $E1^t=176\text{ GPa}$  and  $E1^c=143\text{ GPa}$  while flexure modulus  $E1^f=140\text{ GPa}$ .

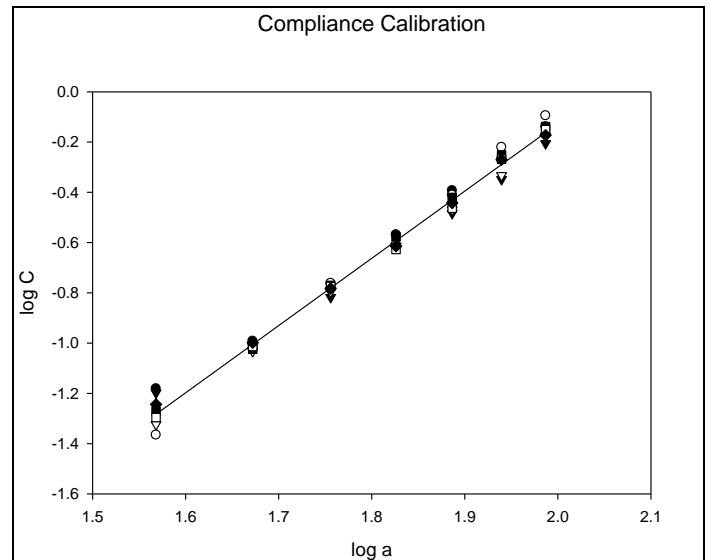


Figure 4 Compliance Calibration curve

The strain energy release rate was estimated using Compliance calibration attributed to Berry. Thus, the strain energy release rate for different crack length was presented in table 1.

**Table 1 Critical Strain Energy release rate**

Crack Length a mm	$G_{IC}$ KJ/m <sup>2</sup>									$G_{IC}$ Average	STD. DEV
	1	2	3	4	5	6	7	8	9		
37	0.231	0.211	0.365	0.275	0.276	0.251	0.272	0.124	0.295	0.266	0.046
47	0.45	0.218	0.454	0.303	0.271	0.261	0.261	0.227	0.316	0.281	0.44
57	0.209	0.210	0.349	0.321	0.287	0.235	0.235	0.224	0.333	0.271	0.054
67	0.209	0.204	0.327	0.361	0.283	0.266	0.266	0.223	0.347	0.278	0.059
77	0.205	0.194	0.355	0.341	0.278	0.267	0.267	0.233	0.351	0.278	0.061
87	0.215	0.191	0.345	0.353	0.268	0.267	0.267	0.234		0.220	0.058
97	0.194	0.192	0.314	0.33	0.261	0.277	0.277	0.233		0.214	0.052

Some factors that affect the DCB test results are loading rate, ambient conditions, the delamination is matrix dominated and is sensitive to cure kinetics. Delamination path is linked to volume fraction, the value of strain energy release rate is sensitive to this phenomenon and this effect is linked to fiber bridging. The nesting or intermingling of the plies indicate that there is distinct interlaminar layer available for the crack propagation and as a result fiber bridging will occur. But in test it was observed there wasn't any distinct layer available for the crack propagation, hence fiber bridging was not observed. After the test the sample was cleaved, and a portion of the sample was machined for SEM examination. The critical energy release rates with crack extension (see Table 2) are almost constant for most of the specimens.

For ENF specimens the test conditions were the same as that of DCB specimens except the cross had speed was 2 mm /min figure 3.

The experimental data was reduced for strain energy release rate using the beam theory and the data for the seven sample were tested, table 2. Pre-cracking was achieved by running the ENF sample under bending fatigue for few cycles when the crack in the resin rich area developed, loading was changed to quasi-static case the resin rich areas at the end of the insert will cause crack blunting and increases the resistance to crack growth. Loading the specimen in three-point fixture will cause the crack to propagate from the edge of the insert to the center of the specimen where it gets arrested by compressive stress, further initial crack length is crucial the correct fracture toughness determination.

**Table 2 Strain Energy release rate in Mode II**

Specimen Thickness mm	DISPLACEMENT mm	Load P <sub>c</sub> N	$G_{IIC}$
3	2.57	798.6	0.6826
3	2.63	827.11	0.7186
3	2.5	764.11	0.6316
3	2.64	875.19	0.7685
3	2.5	808.71	0.6711
3	2.45	755.19	0.6105
3	2.61	842.64	0.7271
		Ave	0.6872
		Std. Dev	0.0555

During mode-II testing the limit load was reached leading to un  $GIC=0.266$  kJ/m<sup>2</sup> and  $GIIC=0.687$  kJ/m<sup>2</sup>. stable crack growth and the crack stopped at the mid span, the parameters load, and the deflection were measured at the beginning of the crack.

## V. SEM CHARACTERIZATIONS

Fracture of continuous fiber/polymer matrix composites usually built up as laminates consisting of individual plies of equal or different orientations can take place in a very complex manner. Within each ply one can find fiber breakage (translaminar fracture) and fracture along the fibers intralaminar fracture). A third type of fracture can occur between individual laminae of equal or different fiber orientation. Several samples were examined under scanning electron microscope. Most of the samples were sputtered and vacuumed to remove the dust flecks. The broken surfaces from the failed samples were scanned. Interlaminar fractures are of special interest because they take place underneath the surface of the laminate structures. Thus, they are not easily detectable, but they can lead to enormous loss in stiffness and strength of the material. The initiation of the cracks can be due to the defects in manufacturing, surface impacts. The major contribution to deformation and fracture is by the polymer matrix and fibers of the individual laminae, whereas only a minor effect can be attributed to fiber fracture events. The reason for the differences in the fracture toughness data can be found in the various failure mechanisms of the polymer matrix and the composite, leading to energy absorbed during the breakdown of the composite under different loading conditions. Fractographic analysis using scanning electron microscope is of great value in this respect.

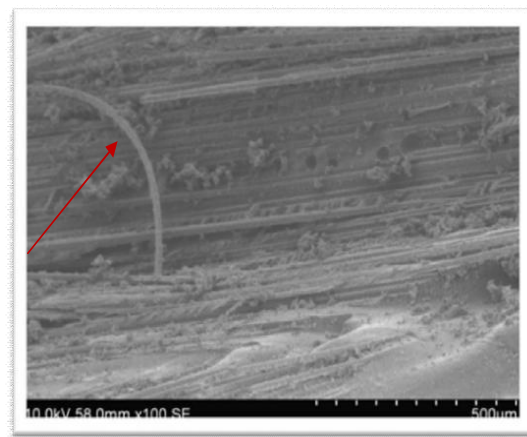


**Figure 5 Mode-I fracture surface appearance represents a typical epoxy system with a ribbon indicated by an arrow**



This typical failure characteristic of Mode-I delamination. It can be observed that a ribbon formed because of the interactions of the fast and slow side of crack propagation.

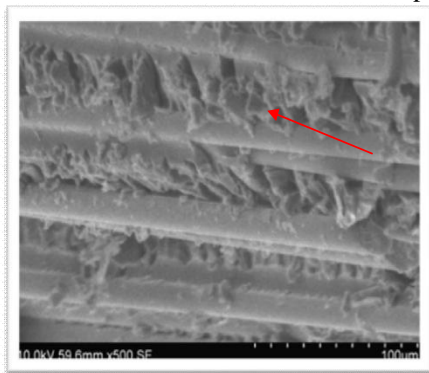


**Figure 6 Mode I Fracture Surface Cusp Formation**

Mode –I failure with a cusp formation which is typical of this mode. No distinction can be made between the fracture surface of the broken samples under very low and high crack opening velocities. The surfaces show carbon fibers with brittle broken epoxy matrix regions between them. Details of fracture sites include the ribbons can be seen and in addition one finds broken fiber ends; partly separated fiber bundles and pieces of broken matrix or fibers which remained somehow attached to the fracture surface Figure 7.

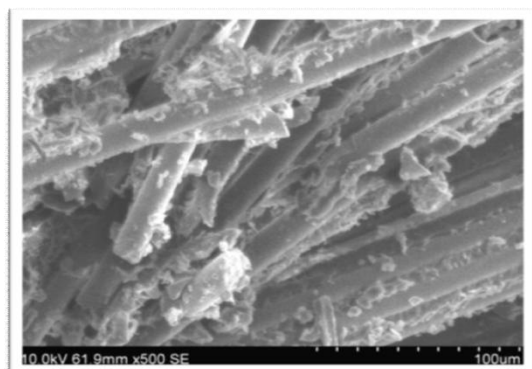


**Figure 7 Fiber bundles and broken matrix**

The existence of numerous pieces of broken matrix under shear type of loading could be shown in figure 8. Much bigger chunks of the matrix material seem to dominate the fracture surface of the broken sample and this may be an indication of a larger extension of the damage region around the propagating crack.

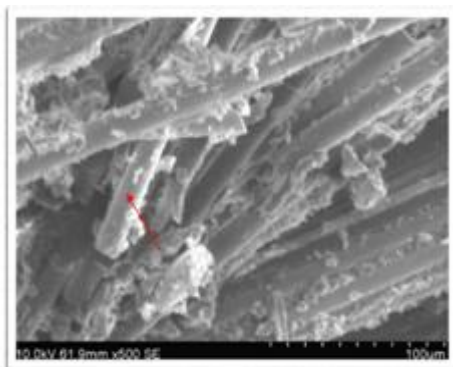


**Figure 8 Mode-II fracture surface with broken fiber indicated by arrow**

Figure 9 shows the typical failure of the ENF samples while testing under Mode-II. It can be observed that the fracture surface has a shear cusp formation which is the characteristic failure under Mode-II loading.

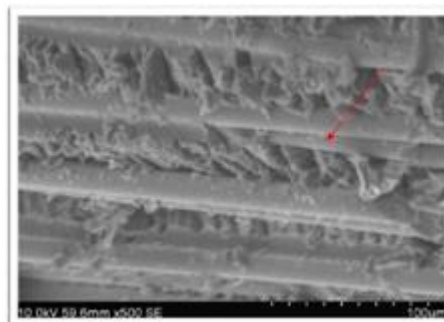


**Figure 9 Mode-II fracture surface with shear cusp indicated by arrow**

## VI. CONCLUSION

The Composite system was characterized for both mode-I and mode-II loading, the data reduction schemes utilized the beam theory while estimating the compliance, care was taken to estimate the moduli. Fiction between the insets and the plies were assumed to be absent. The reason for not observing the fiber bridging could be attributed to the volume fraction, intermingling of plies and there was no distinct layer for the crack to propagate. While the strain energy release rate in mode-II are obtained by using the compliance calibration starting from beam theory, insert length is essential for correct determination of the fracture toughness. The values were found to be  $G_{IC}=0.266 \text{ kJ/m}^2$  and

$$G_{IIC}=0.687 \text{ kJ/m}^2.$$

The current work can be extended to disperse various filler materials and characterize it for different loading including mode-III and mixed mode behavior,

## ACKNOWLEDGEMENT

The author would like to thank the management for providing the facilities to test the samples. The SEM analysis was obtained from Hitachi Scanning Electron microscopy system at SAIF, in IIT (m).

## REFERENCES

1. John M Barsom, Stanley, T Rolfe. (1987). Fracture and Fatigue control in structures: Application of Fracture Mechanics. Second Edition. Prentice Hall.Inc. USA.
2. Berry. J. (1963). Deformation of Fracture Surface by Cleavage Technique. J. Appl. Phys. 31,62
3. Todd M Mower, Victor C Li. (1987). Fracture characterization of random short fiber reinforced thermoset resin composites. Engineering fracture Mechanics. **26**(4):593-603.
4. C K H Dharan. (1978). Fracture mechanics of composite materials. Journal of engineering materials and technology. 100: 223-247.
5. Reeder J R. (1993). A Bilinear Failure Criterion for Mixed-Mode Delamination. composite Materials: Testing and Design, ASTM STP 1206, E.T. Camponeschi, Jr., Ed. ASTM Int., W. Conshohocken, PA. **11**: 303-322.
6. O'Brien T. K., and Martin R. H. (1993). Results of ASTM Round Robin Testing for Mode I Interlaminar Fracture Toughness of Composite Materials. Journal of Composites Technology and Research. **15**(4): 269 –281.
7. A B de Morais. (2003). Double cantilever beam testing of multidirectional



- laminates. Composite Part A: Applied Science. **A34**(12):1135–1142.
8. Pereira A B, de Morais A B. (2004). Mode I interlaminar fracture of carbon/epoxy multidirectional laminates. Composite Science and Technology. **64**:2261–2270.
  9. Choi N S, Kinloch A J, Willams J G. (1999). Delamination fracture of multidirectional carbon-fiber / epoxy composites under mode I, mode II and mixed mode I/II loading. Journal of Composite Material. **33**(1):73–100.
  10. A J Brunner, B R K Blackman and P Davies. (2008). A status report on delamination resistance testing of polymer–matrix composites. Engineering Fracture Mechanics. **75**: 2779–2794.
  11. Davies P. (1993). ESIS protocols for interlaminar fracture testing of composites. France, IFREMER brochure.
  12. O'Brien T K. (1998). Interlaminar fracture toughness: the long and winding road to standardization. Composites- Part B: Engineering. **29B**(1):57–62.
  13. Gibson R F. (1994). Principles of Composite Material Mechanics. McGraw Hill, USA: 395-

### AUTHOR PROFILE



**J. V. Sai Prasanna Kumar** graduated from IIT (M) in Aerospace Engineering and obtained doctorate from Anna University in Composite materials. NDT, Fracture Mechanics and Composite Materials are his specializations.